

A hybrid type Ia supernova with an early flash triggered by helium-shell detonation

Ji-an Jiang^{1,2}, Mamoru Doi^{1,3,4}, Keiichi Maeda^{5,3}, Toshikazu Shigeyama⁴, Ken'ichi Nomoto³, Naoki Yasuda³, Saurabh W. Jha⁶, Masaomi Tanaka^{7,3}, Tomoki Morokuma^{1,3}, Nozomu Tominaga^{7,3}, Željko Ivezić⁹, P. Ruiz-Lapuente^{10,11}, M. D. Stritzinger¹², P. A. Mazzali^{13,14}, Christopher Ashall¹³, Jeremy Mould¹⁵, D. Baade¹⁶, Nao Suzuki³, Andrew J. Connolly⁹, F. Patat¹⁶, Lifan Wang^{17,18}, Peter Yoachim⁹, David Jones^{19,20}, Hisanori Furusawa⁷, Satoshi Miyazaki^{7,21}

¹*Institute of Astronomy, Graduate School of Science, The University of Tokyo, 2-21-1 Osawa, Mitaka, Tokyo 181-0015, Japan*

²*Department of Astronomy, Graduate School of Science, The University of Tokyo, 7-3-1 Hongo, Bunkyo-ku, Tokyo 113-0033, Japan*

³*Kavli Institute for the Physics and Mathematics of the Universe (WPI), The University of Tokyo, 5-1-5 Kashiwanoha, Kashiwa, Chiba 277-8583, Japan*

⁴*Research Center for the Early Universe, Graduate School of Science, The University of Tokyo, 7-3-1 Hongo, Bunkyo, Tokyo 113-0033, Japan*

⁵*Department of Astronomy, Kyoto University, Kitashirakawa-Oiwake, Sakyo, Kyoto 606-8502, Japan*

⁶*Department of Physics and Astronomy, Rutgers, The State University of New Jersey, 136 Frelinghuysen Road, Piscataway, NJ 08854, USA*

⁷*National Astronomical Observatory of Japan, 2-21-1 Osawa, Mitaka, Tokyo 181-8588, Japan*

⁸*Department of Physics, Faculty of Science and Engineering, Konan University, 8-9-1 Okamoto, Kobe, Hyogo 658-8501, Japan*

⁹*Department of Astronomy, University of Washington, Box 351580, Seattle, WA 98195-1580,*

USA

¹⁰*Instituto de Física Fundamental, Consejo Superior de Investigaciones Científicas, c/. Serrano 121, E-28006, Madrid, Spain*

¹¹*Institut de Ciències del Cosmos (UB-IEEC), c/. Martí i Franqués 1, E-08028, v, Spain*

¹²*Department of Physics and Astronomy, Aarhus University, Ny Munkegade 120, 8000 Aarhus C, Denmark*

¹³*Astrophysics Research Institute, Liverpool John Moores University, IC2, Liverpool Science Park, 146 Brownlow Hill, Liverpool L3 5RF, UK*

¹⁴*Max-Planck-Institut für Astrophysik, Karl-Schwarzschild-Str. 1, D-85748 Garching, Germany*

¹⁵*Centre for Astrophysics and Supercomputing, Swinburne University of Technology, Hawthorn, Vic 3122, Australia*

¹⁶*European Organisation for Astronomical Research in the Southern Hemisphere (ESO), Karl-Schwarzschild-Str. 2, 85748 Garching b. München, Germany*

¹⁷*George P. and Cynthia Woods Mitchell Institute for Fundamental Physics Astronomy, Texas A. M. University, Department of Physics and Astronomy, 4242 TAMU, College Station, TX 77843, USA*

¹⁸*Purple Mountain Observatory, Chinese Academy of Sciences, Nanjing 210008, China*

¹⁹*Instituto de Astrofísica de Canarias, E-38205 La Laguna, Tenerife, Spain*

²⁰*Departamento de Astrofísica, Universidad de La Laguna, E-38206 La Laguna, Tenerife, Spain*

²¹*SOKENDAI (The Graduate University for Advanced Studies), Mitaka, Tokyo, 181-8588, Japan*

Type Ia Supernovae (SNe Ia) arise from the thermonuclear explosion of carbon-oxygen white dwarfs^{1,2}. Though the uniformity of their light curves makes them powerful cosmological distance indicators^{3,4}, long-standing issues remain regarding their progenitors and explosion mechanisms^{2,5,6}. Recent detection of the early ultraviolet pulse of a peculiar subluminescent SN Ia has been claimed as new evidence for the companion-ejecta interaction through the single-degenerate channel^{7,8}. Here, we report the discovery of a prominent but red optical flash at ~ 0.5 days after the explosion of a SN Ia which shows hybrid features of different SN Ia sub-classes: a light curve typical of normal-brightness SNe Ia, but with strong titanium absorptions, commonly seen in subluminescent SN Ia spectra. We argue that the early flash of such a hybrid SN Ia is different from predictions of previously suggested scenarios such as the companion-ejecta interaction^{8–10}. Instead it can be naturally explained by a SN explosion triggered by a detonation of a thin helium shell either on a near-Chandrasekhar-mass white dwarf ($\gtrsim 1.3 M_{\odot}$) with low-yield ^{56}Ni or on a sub-Chandrasekhar-mass white dwarf ($\sim 1.0 M_{\odot}$) merging with a less massive secondary. This finding provides compelling evidence that one branch of the proposed explosion models, the Helium-ignition scenario, does exist in nature, and such a scenario may account for explosions of white dwarfs in a wider mass range in contrast to what was previously supposed^{11–14}.

A faint optical transient was discovered on UT April 4th, 2016 through the newly established high-cadence deep-imaging survey which is optimized for finding Type Ia Supernovae (SNe Ia) within a few days after explosion with the Subaru/Hyper Suprime-Cam (HSC)¹⁵—“the **MU**lti-

band Subaru Survey for Early-phase SNe Ia” (MUSSES). Close attention has been paid to one transient because its brightness increased by ~ 6.3 times within 20 hours of the first observation. We designated this fast-rising transient as MUSSES1604D (the official ID is SN 2016jhr), the fourth early-phase SN candidate found in the April 2016 observing run of MUSSES.

Figure 1 presents the observed g -, r -, i -band light curves of MUSSES1604D. The earliest photometry by Subaru/HSC indicates an apparent g -band magnitude of 25.14 ± 0.15 on April 4 (MJD 57482.345). One day later, MUSSES1604D rapidly brightened to ~ 23.1 and 23.0 mag in the g and r bands, respectively. More surprisingly, the g -band observation on April 6 indicates that the transient “paused” brightening from April 5 and shows plateau-like evolution lasting for ~ 1 day. At the same time, the transient also slowed down in its rate of brightening in the r band.

Follow-up observations indicated that MUSSES1604D is a SN Ia with a r -band peak absolute magnitude of ~ -19.1 on April 26. Adopting a host galaxy redshift z of 0.11737, the rest-frame light curves in the B - and V -band absolute magnitudes from ~ 4 days after the first observation are derived by applying a K-correction based on the best-fitting model with SALT2¹⁶. Because of the peculiar flash at early time, K-correction for the flash-phase light curves is performed by simplified spectral energy distributions estimated from the early color information of MUSSES1604D (see Methods). The rest-frame B -band light curve shows a peak absolute magnitude of -18.8 and $\Delta m_{15}(B) \approx 1.0$ mag, indicating a normal-brightness SN Ia¹⁷.

Color evolution within a few days after the SN explosion is crucial for identifying the early

flash^{8,10}. In contrast to another peculiar early-flash SN Ia iPTF14atg with $B - V$ color evolution obtained only from ~ 5 days after the discovery⁷, the specific survey strategy of the MUSSES project enables us to obtain the color information of MUSSES1604D from ~ 1 day after our first observation (Figure 2), which shows a $B - V$ color of ~ 0.1 mag at first, and rapidly reddens to ~ 0.4 mag in one day.

The interaction of SN ejecta with a non-degenerate companion star^{8,18,19} (companion-ejecta interaction, CEI) or with dense circumstellar material^{9,10} (CSM-ejecta interaction) are popular scenarios to explain the early optical flash. In order to produce a prominent optical flash comparable to that of MUSSES1604D, either a companion with a very extended envelope or a large-scale CSM distribution is required. In the CEI scenario, a prominent flash generated from the inner hot region of ejecta can be observed through the hole which is carved by a red-giant companion^{8,19}. In the CSM-ejecta-interaction scenario, a more extended CSM distribution could generate a brighter flash but with longer diffusion time. Our best-fitting CEI model (Figure 2 & 3) and previous simulations of both two scenarios^{8,10,19} all indicate that the particular blue color evolution is inevitable when producing the early flash as bright as that of MUSSES1604D (Extended Data Figure 1), which is incompatible with the red and rapid early color evolution observed for MUSSES1604D.

Peculiar spectral features have been discovered around the peak epoch (Figure 4). At a first glance, the Si II $\lambda 6355$ line, “W”-shape S II feature, and Ca II H & K absorptions are reminiscent of a normal SN Ia, while the weak Si II $\lambda 5972$ line indicates a higher photospheric temperature compared to those of SNe Ia with similar luminosities. On the other hand, prominent

absorption features such as the Ti II trough around 4150 Å, usually attributed to low temperature, have been found at the same time, in contrast to the brightness indicated by the light curve. By inspection of near-maximum spectra of over 800 non-subluminous SNe Ia, we found three MUSSES1604D-like SNe Ia—SN 2006bt, SN 2007cq, and SN 2012df (Extended Data Figure 2 & 3). This fraction of $\sim 0.5\%$ indicates the rarity of such hybrid SNe Ia.

The peculiar spectral features and the early flash followed by a normal-brightness light curve observed for MUSSES1604D are incompatible with predictions of classical explosion mechanisms^{20,21} through the hydrogen-accreting single degenerate channel, but suggested by a specific scenario in which the SN explosion is triggered by the He-shell detonation, so-called the double-detonation (DDet) scenario^{12,13,22,23}. In principle, a He-shell detonation not only generates a shock wave propagating toward the center of the white dwarf (WD) and ignites carbon burning near the center, but also allocates ^{56}Ni and other radioactive isotopes such as ^{52}Fe and ^{48}Cr to the outermost layers where the optical depth is relatively low^{12,23}. Therefore energy deposited by decaying radioactive isotopes diffuses out and consequently results in a prominent flash in the first few days after the explosion (see Methods). Observationally, the plateau-like light curve enhancement can be observed with the day-cadence observations. At the same time, a significant amount of not only iron group elements but also intermediate mass elements such as Ti and Ca will be produced in the outermost layers^{12,13,23}. Vast numbers of absorption lines of these elements are very effective in blocking the flux in the blue part of the spectrum, thus leading to a relatively red $B - V$ color evolution in general. Indeed, while a substantial amount of He is left after the detonation, the expected spectrum would not show a trace of He in the optical²⁴. By assuming a progenitor star with a WD mass of $1.03 M_{\odot}$ and a He-shell mass

as low as $\sim 0.054 M_{\odot}$ (as required to trigger the He detonation on the surface of a $1.03 M_{\odot}$ WD^{12,23}), the prominent early flash, peculiar early color evolution and Ti II trough feature are reproduced simultaneously (Figures 2–4). The similar early-phase photometric behavior found in our simulation has also been independently shown by a simulation of the sub-Chandrasekhar DDet model by another group very recently²⁵, showing the validity of our simulation and interpretation.

A potential issue in our simulation is the assumption of a sub-Chandrasekhar-mass WD with a thin He-shell. The amount of synthesized ^{56}Ni is sensitive to the mass of the exploding WD and determines the peak luminosity^{12,23}. The DDet model requires a sub-Chandrasekhar-mass WD ($\sim 1 M_{\odot}$) for the peak luminosity of MUSSES1604D. However, DDet happening on such a WD would lead to a fast-evolving *B*-band light curve, which is inconsistent with a much slower-evolving light curve observed for MUSSES1604D. In addition, an early flash resulting from the corresponding He mass of $0.054 M_{\odot}$ is too bright. We suggest two alternative scenarios that also involve He detonation to solve this issue. A He-ignited violent merger¹⁴ can easily trigger a detonation in a thin He shell, and could produce the light curve of MUSSES1604D, but by fine-tuning the configuration of the binary system. Whether core detonation can be triggered by the thin-He-shell detonation through the double-degenerate channel is also an open question^{26,27}. Alternatively, the lower mass He can be detonated on the surface of a near-Chandrasekhar-mass WD, which provides a better and more straightforward account of the light curve and spectral features (Figures 2–4). Further investigation suggests that the best-fitting WD mass is in the range of $1.28\text{--}1.38 M_{\odot}$ but with a low-yield ^{56}Ni compared with the prediction by DDet (see Methods). This suggests that there could be a mechanism to reduce the mass of ^{56}Ni in the

explosion triggered by the He detonation. For example, the shock wave generated by the He detonation may trigger a deflagration rather than a detonation near the center of the WD²⁸ due to the high degeneracy pressure inhibiting the formation of a shock wave as strong as the sub-Chandrasekhar-mass WD counterpart. Though the observed peculiarities of MUSSES1604D can be naturally explained by this scenario, how a thin He-shell is formed on such a massive WD during the binary evolution still requires further investigation.

The discovery of MUSSES1604D indicates that the He-detonation-triggered scenario is also promising to explain early-flash SNe Ia in addition to other “popular” scenarios^{8–10}. The prominent optical excess and peculiar color evolution in the earliest phase together with absorptions due to Ti II ions in around-max spectra can be used as indicators of this scenario. The slow-evolving *B*-band light curve makes the classical sub-Chandrasekhar DDet model previously supposed^{11,12} unlikely. Recent work shows that the sub-Chandrasekhar DDet scenario could explain a part of normal SNe Ia if only a negligible amount of He exists at the time of the He-shell detonation^{29,30}. Given that MUSSES1604D is best explained by a thin He-shell but still more massive than required in the above scenario, it opens up a possibility that the He-detonation-trigger scenario would produce a range of observational counterparts, controlled by the masses of both the WD and the He shell. The discovery of MUSSES1604D thus provides the first observational calibration about the range and combination of these quantities realized in nature.

1. Filippenko, A. V. Optical Spectra of Supernovae. *Ann. Rev. Astron. Astrophys.* **35**, 309–355 (1997).
2. Maoz, D., Mannucci, F. & Nelemans, G. Observational Clues to the Progenitors of Type Ia Supernovae. *Ann. Rev. Astron. Astrophys.* **52**, 107–170 (2014).
3. Perlmutter, S., *et al.* Measurements of Ω and Λ from 42 High-Redshift Supernovae. *Astrophys. J.* **517**, 565–586 (1999).
4. Riess, A. G., *et al.* Observational Evidence from Supernovae for an Accelerating Universe and a Cosmological Constant. *Astron. J.* **116**, 1009–1038 (1998).
5. Hillebrandt, W. & Niemeyer, J. C. Type IA Supernova Explosion Models. *Ann. Rev. Astron. Astrophys.* **38**, 191–230 (2000).
6. Whelan, J. & Iben, I., Jr. Binaries and Supernovae of Type I. *Astrophys. J.* **186**, 1007–1014 (1973).
7. Cao, Y. *et al.* A strong ultraviolet pulse from a newborn type Ia supernova. *Nature.* **521**, 328–331 (2015).
8. Kasen, D. Seeing the Collision of a Supernova with Its Companion Star. *Astrophys. J.* **708**, 1025–1031 (2010).
9. Levanon, N., Soker, N. & García-Berro, E. Constraining the double-degenerate scenario for Type Ia supernovae from merger ejected matter. *Mon. Not. Astron. Roy. Soc.* **447**, 2803–2809 (2015).
10. Piro, A. L. & Morozova, V. S. Exploring the Potential Diversity of Early Type Ia Supernova Light Curves. *Astrophys. J.* **826**, 96 (2016).
11. Bildsten, L., Shen, K. J., Weinberg, N. N. & Nelemans, G. Faint Thermonuclear Supernovae from AM Canum Venaticorum Binaries. *Astrophys. J. Lett.* **662**, L95–L98 (2007).
12. Fink, M., *et al.* Double-detonation sub-Chandrasekhar supernovae: can minimum helium shell masses detonate the core? *Astron. & Astrophys.* **514**, 53 (2010).
13. Woosley, S. E. & Kasen, D. Sub-Chandrasekhar Mass Models for Supernovae. *Astrophys.*

J. Lett. **747**, 38 (2011).

14. Pakmor, R., Kromer, M., Taubenberger, S. & Springel, V. Helium-ignited Violent Mergers as a Unified Model for Normal and Rapidly Declining Type Ia Supernovae. *Astrophys. J. Lett.* **770**, L8 (2013).

15. Miyazaki, S., *et al.* Hyper Suprime-Cam. *SPIE*, **8446**, 84460Z-1–84460Z-9 (2012).

16. Guy, J., *et al.* SALT2: using distant supernovae to improve the use of type Ia supernovae as distance indicators. *Astron. & Astrophys.* **466**, 11–21 (2007).

17. Phillips, M. M. The absolute magnitudes of Type IA supernovae. *Astrophys. J. Lett.* **413**, L105–L108 (1993).

18. Pan, K., Ricker, P. M. & Taam, R. E. Impact of Type Ia Supernova Ejecta on Binary Companions in the Single-degenerate Scenario. *Astrophys. J.* **750**, 151 (2012).

19. Kutsuna, M. & Shigeyama, T. Revealing progenitors of type Ia supernovae from their light curves and spectra. *Publ. Astron. Soc. Jap.* **67**, 54 (2016).

20. Nomoto, K., Thielemann, F. -K. & Yokoi, K. Accreting white dwarf models for type I supern. III. Carbon deflagration supernovae. *Astrophys. J.* **286**, 644–658 (1984).

21. Khokhlov, A. M. Delayed detonation model for type IA supernovae. *Astron. & Astrophys.* **245**, 114–128 (1991).

22. Guillochon, J., Dan, M., Ramirez-Ruiz, E. & Rosswog, S. Surface Detonations in Double Degenerate Binary Systems Triggered by Accretion Stream Instabilities. *Astrophys. J. Lett.* **709**, L64–L69 (2010).

23. Kromer, M., *et al.* Double-detonation Sub-Chandrasekhar Supernovae: Synthetic Observables for Minimum Helium Shell Mass Models. *Astrophys. J.* **719**, 1067–1082 (2010).

24. Boyle, A., Sim, S. A., Hachinger, S. & Kerzendorf, W. Helium in Double-Detonation Models of Type Ia Supernovae. *Astron. & Astrophys.* **599**, 46 (2017).

25. Noebauer, U. M., *et al.* Early light curves for Type Ia supernova explosion models. Preprint at (<http://arxiv.org/abs/1706.03613>) (2017).

26. Shen, K. J. & Bildsten, L. The Ignition of Carbon Detonations via Converging Shock Waves in White Dwarfs. *Astrophys. J.* **785**, 61 (2014).
27. Tanikawa, A., *et al.* Hydrodynamical Evolution of Merging Carbon-Oxygen White Dwarfs: Their Pre-supernova Structure and Observational Counterparts. *Astrophys. J.* **807**, 40 (2015).
28. Nomoto, K., Sugimoto, D. & Neo, S. Carbon Deflagration Supernova, an Alternative to Carbon Detonation. *Astrophys Space Sci.* **39**, L37–L42 (1976).
29. Blondin, S., Dessart, L., Hillier, D. J. & Khokhlov, A. M. Evidence for sub-Chandrasekhar-mass progenitors of Type Ia supernovae at the faint end of the widthluminosity relation. *Mon. Not. Astron. Roy. Soc.* **470**, 157–165 (2017).
30. Shen, K. J., Kasen, D., Miles, B. J. & Townsley, D. M. Sub-Chandrasekhar-mass white dwarf detonations revisited. Preprint at (<http://arxiv.org/abs/1706.01898>) (2017).

Author Contributions J.J. initiated the study, conducted analysis and wrote the manuscript as the PI of the MUSSES project. M.D. contributed to the initiation of the MUSSES project, and assisted with the manuscript preparation and the analysis together with K.M. and T.S. K.M. and T.S. organized the efforts for the theoretical interpretation with J.J. and M.D. K.M. investigated the He-detonation-triggered explosion models and conducted radiative transfer calculations used to generate simulated light curves and spectra. T.S. developed and ran the radiative transfer calculations used to generate simulated CEI-induced light curves. K.N. provided insights into the He-detonation-triggered explosion models and assisted with the analysis. N.Y., H.F. and M.S. are core software developers for HSC and in charge of the HSC SSP project. N.Y. also developed the HSC transient server with N.T. and M.T. for the real-time candidates selection and contributed to the Subaru/HSC observation and data reduction. T.M. contributed to the Subaru/HSC observation and the Kiso/KWFC ToO observation. S.W.J. contributed to the SALT spectroscopies and data reduction. Z.I., A.C., P.Y., P.R-L., N.S., F.P., D.B., J.M., L.W., M.D.S., D.J., P.A.M. and C.A. are core collaborators of the MUSSES project who are in charge of follow-up observations (including proposal preparations) with ARC, GTC, VLT, NOT, INT and LT. All the authors contributed to discussions.

Author Information The authors declare no competing financial interests. Correspondence and requests for materials should be addressed to J.J. (email: yuzhoujiang@ioa.s.u-tokyo.ac.jp).

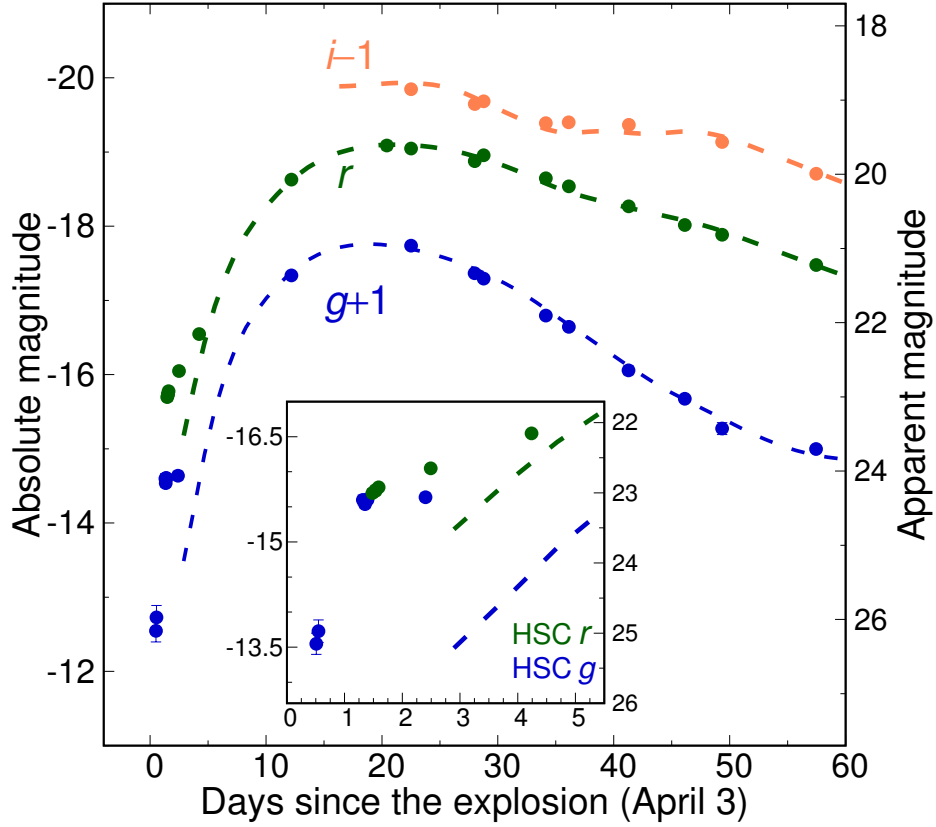


Figure 1: The multi-band light curve of MUSSES1604D. Photometry in g , r and i bands (observer-frame) are in the AB system. The error bars denote $1-\sigma$ uncertainties. Dashed lines in g , r and i bands are best-fitting light curves derived from the non-early photometry ($t \gtrsim 12$ days) with SALT2¹⁶. The explosion epoch is estimated by adopting a classical t^2 fireball model for the early-flash phase (see Methods). The inset zooms in on the early-phase multi-band light curve by Subaru/HSC, which shows that the brightening in g -band “paused” after the second-night observation.

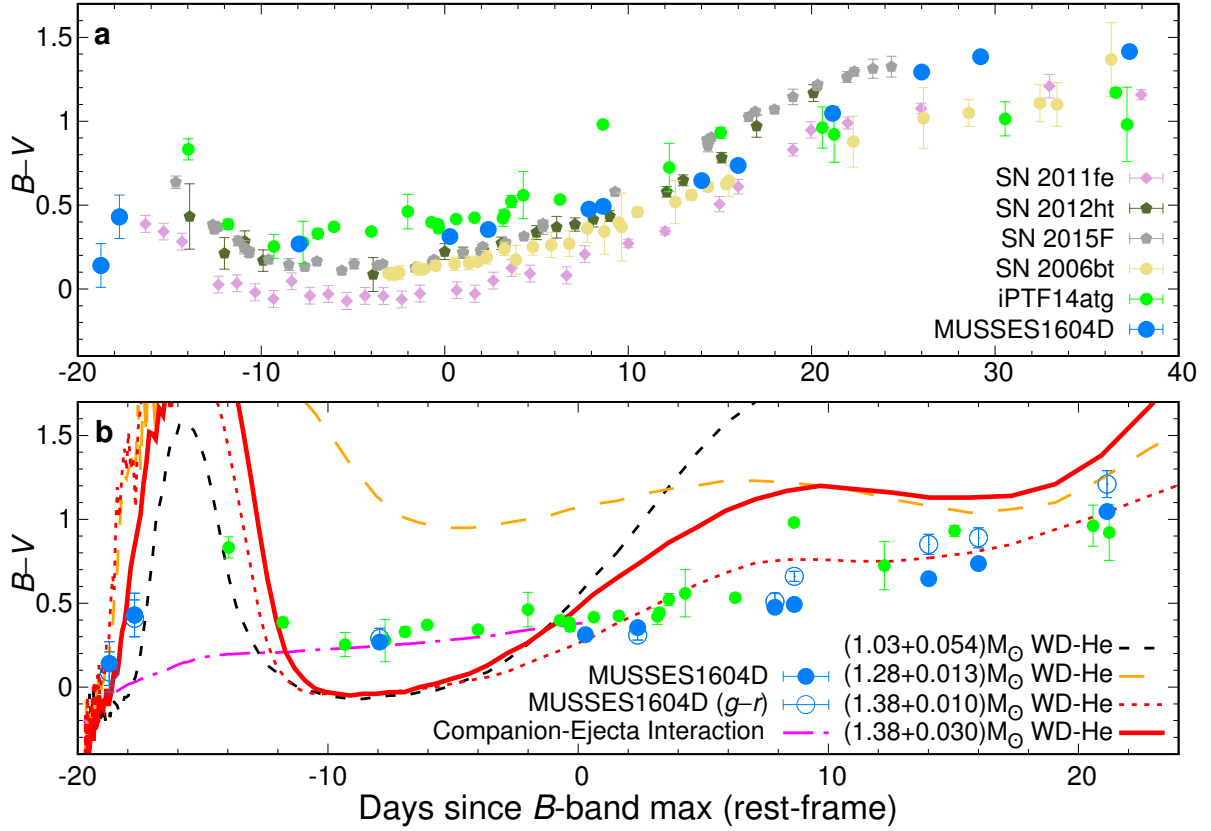


Figure 2: Comparative analysis of MUSSES1604D color evolution. The upper panel presents $B - V$ color evolution of MUSSES1604D, iPTF14atg, SN 2006bt (MUSSES1604D-like), SN 2012ht (transitional), SN 2015F and SN 2011fe (normal). The lower panel shows the color evolution predicted by CEI, He-detonation model for the sub-Chandrasekhar-mass WD and the newly proposed He-detonation models for the near-Chandrasekhar-mass WD under different He-shell mass assumptions. The date of B -band maximum is ~ 20 days after the explosion. As the bandpass difference between the rest-frame B/V band and the observer-frame g/r band is inconspicuous at $z \sim 0.1$, the observed $g - r$ color evolution is provided for reference. Error bars represent $1-\sigma$ uncertainties.

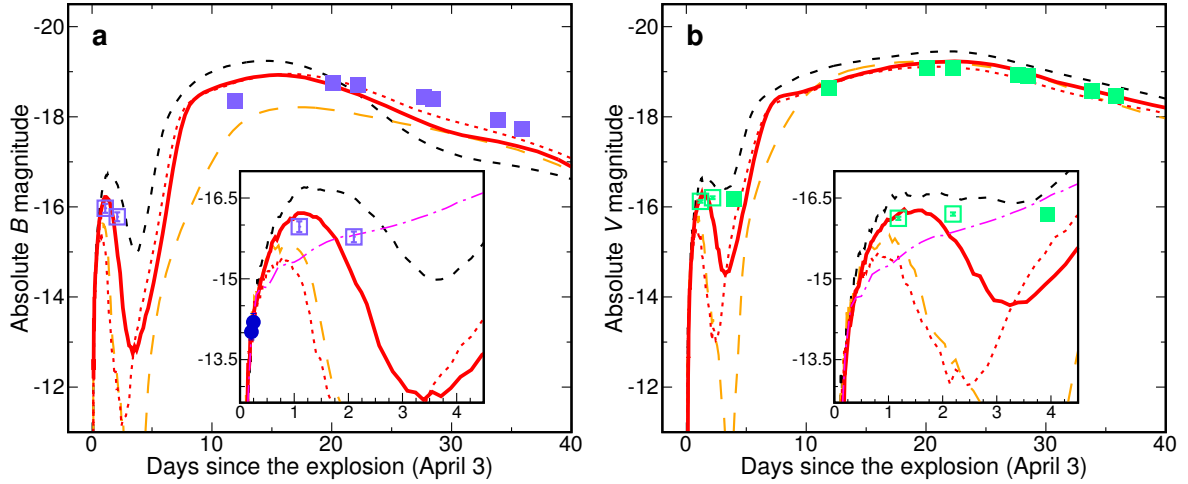


Figure 3: Rest-frame B - and V -band light curves of MUSSES1604D and simulations. K -corrections in the flash (open squares) and the post-flash phase (solid squares) are carried out with different methods. Each panel includes He-detonation models for sub-Chandrasekhar-mass WD ($1.03 M_{\odot}$ WD + $0.054 M_{\odot}$ He-shell; black dashed line) and massive WD ($1.28 M_{\odot}$ WD + $0.013 M_{\odot}$ He-shell, orange long-dashed line; $1.38 M_{\odot}$ WD + $0.01 M_{\odot}$ He-shell, red dotted line; $1.38 M_{\odot}$ WD + $0.03 M_{\odot}$ He-shell, red solid line) conditions. The inset zooms in on the flash phase and also includes our best-fitting CEI model assuming a $1.05 M_{\odot}$ red-giant companion (magenta dash-dot line). The first-night g -band data (blue circles) are included in panel **a**. Error bars denote $1\text{-}\sigma$ uncertainties.

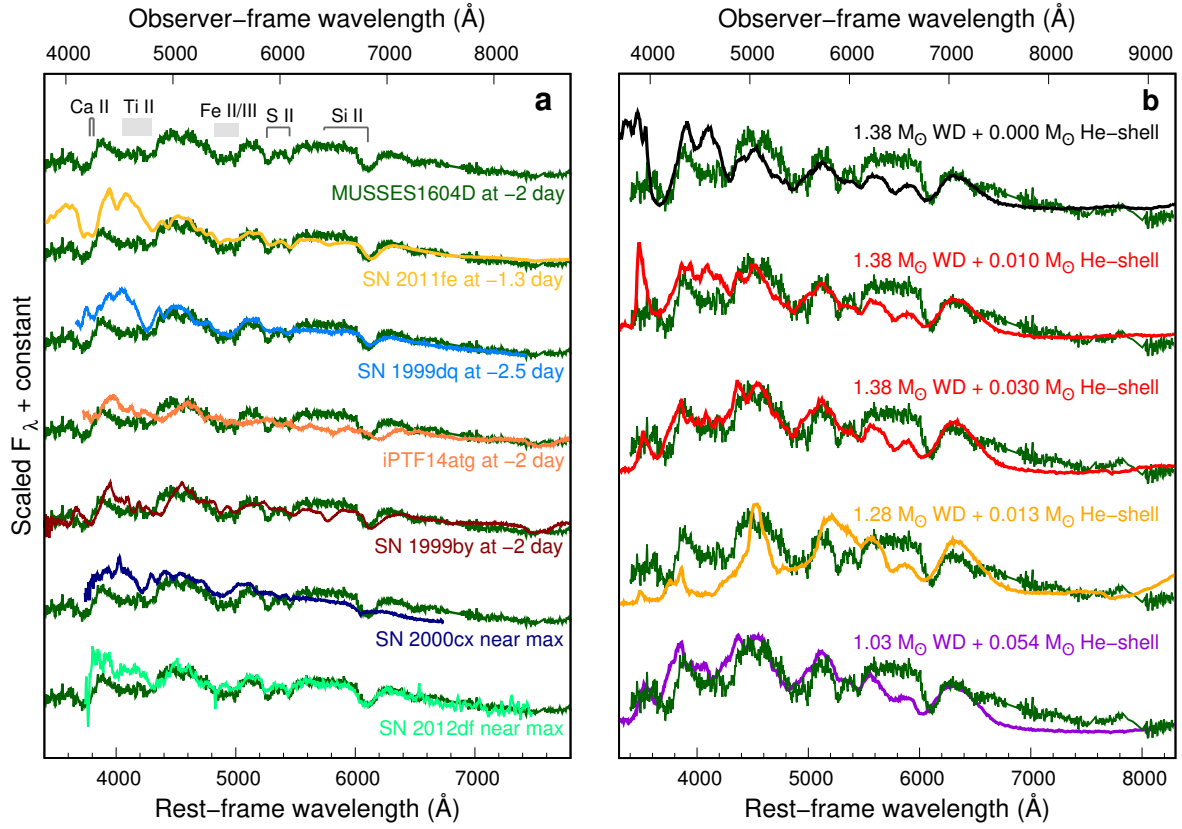


Figure 4: The around-maximum spectral comparison between MUSSES1604D, other observed SNe Ia of different types, and models. In panel **a**, the spectrum of MUSSES1604D taken 2 days before the *B*-band maximum by SALT is compared with that of SN 2011fe (normal), SN 1999dq (shallow-silicon), SN 1999by (subluminous), iPTF14atg (early-flash) and SN 2012df (MUSSES1604D-like) at similar epoch. Major absorption features are labeled on the spectrum of MUSSES1604D. In panel **b**, simulated spectra of the classical W7 deflagration model, the newly proposed He-detonation models with different He-shell mass assumptions and the classical double-detonation model for the sub-Chandrasekhar-mass WD are compared with MUSSES1604D at the same epoch.

Methods

I. The Handbook for MUSSES1604D

The MUSSES project and the discovery of MUSSES1604D The Subaru Hyper Suprime-Cam¹⁵ (HSC) is a new generation large field camera which started to serve as a facility instrument of the 8.2-m Subaru telescope for open-use from 2014. With a total of 116 CCDs, a single HSC pointing covers 1.8 square degrees and reaches to a g -band limiting magnitude ($5\text{-}\sigma$) of about 26.5 mag with exposure time of 300 s.

The **MU**lti-band **S**ubaru **S**urvey for **E**arly-phase **S**Ne Ia (**MUSSES**) is a newly established project which aims to systematically investigate the photometric and spectroscopic behavior of SNe Ia within a few days after their explosions (hereafter Early-phase SNe Ia, ESNe Ia) with Subaru/HSC and other 1–10 m class telescopes around the world. In every semester, we plan to carry out 1–2 observing runs and each of them includes two stages: the Subaru/HSC survey (2–3 nights) and follow-up observations. For the survey stage, Subaru/HSC observes over 100 square degrees of sky with a g -band limiting magnitude of 26.0 ($5\text{-}\sigma$) every night for finding ESNe Ia and obtaining their multi-band light curve information. Using the HSC transient pipeline and newly employed machine-learning classifiers, we are able to carry out real-time candidate selection during the survey and trigger photometric/spectroscopic follow-ups within one day after the Subaru observation. Because of the fast brightening of ESNe Ia, photometric follow-up observations can be conducted well with 1–4 m telescopes. The strategy of MUSSES gives a very large photometric dynamic range, enabling us to observe ESNe Ia

even reaching to redshift $z \sim 0.3$.

In order to make the best use of the Subaru time, the MUSSES observing run in April 2016 adopted a specific survey mode which combines both HSC Subaru Strategic Program (HSC SSP³¹, 1-night g -band observation, from UT 2016 April 4.17 to UT 2016 April 4.67) and open-use observation (1.5-nights g - and r -band observation, from UT 2016 April 5.17 to 5.67 and April 6.43 to 6.67 respectively).

The supernova MUSSES1604D (official ID: SN 2016jhr) was discovered on UT 2016 April 4.345 at $\alpha(\text{J2000}) = 12\text{h}18\text{m}19\text{s}.85$ and $\delta(\text{J2000}) = +00^\circ 15' 17.38''$ with a g -band magnitude of 25.14 mag upon discovery (Extended Data Figure 4), and was the fourth ESN candidate found in the April observing run. MUSSES1604D was located about $5.8''$ (to the southwest) from the host galaxy. The redshift of the host galaxy is 0.11737 ± 0.00001 according to the SDSS (Data Release 12)³². With cosmological parameters $H_0 = 70 \text{ km s}^{-1} \text{ Mpc}^{-1}$, $\Omega_m = 0.30$, $\Omega_\Lambda = 0.70$ and $\Omega_v = 0.00$, we calculate a luminosity distance of 546.5 megaparsecs and a distance modulus of 38.67 mag for MUSSES1604D.

The host galaxy The red color with a visible $\text{H}\alpha$ emission feature suggests that the host galaxy of MUSSES1604D is a star-forming early type galaxy³³. Further analysis of the SDSS photometry and spectroscopy shows the semi major axis of the host is ~ 27.9 kiloparsecs and the stellar mass is $\sim 2.8 \times 10^{10} M_\odot$, which is also consistent with an early type galaxy, e.g. an S0 galaxy.

Follow-up observations Our scheduled early follow-up observations at La Palma island and Apache Point Observatory were lost due to poor weather conditions. Fortunately, HSC SSP *r*-band observation conducted in two days after our Subaru/HSC observations successfully took another *r*-band image of MUSSES1604D, which provides a crucial constraint on the timescale of the early-flash. Multi-band follow-up observations with the 8.2-m Gemini-North telescope, the 3.5-m ARC telescope, the 2.5-m Nordic Optical Telescope (NOT), the 2.5-m Isaac Newton Telescope (INT), the 2-m Liverpool Telescope (LT) and the 1.05-m Kiso Schmidt telescope have been conducted from about -8 days to +40 days after the *B*-band maximum. For the spectroscopic observations, we triggered the 9.2-m SALT telescope and the 8.2-m Gemini-North telescope at specific epochs to get spectral evolution from about -2 days to one month after the *B*-band maximum (Extended Data Figure 2).

Data reduction and photometric calibration As MUSSES1604D resides at the edge of the host galaxy, contamination from the host is negligible except for the photometry of the earliest Subaru/HSC observation. The morphology of the host galaxy indicates a symmetric S0 galaxy. We thus built the host template with GALFIT^{34,35} and performed the standard point spread function (PSF) photometry with the IRAF DAOPHOT package³⁶ on host-subtracted images. The photometry has been tested by subtracting the SN from the original image using an artificial PSF star with the derived photometric magnitude. The average flux of the residual region is comparable with the surrounding region and well below the photometric error of the discovery image by Subaru ($\Delta m \approx 0.14$ mag). PSF photometry is performed on host-subtracted images for all follow-up observations. The photometry is then calibrated to the standard SDSS photometric system by adopting a color term correction based on field stars³⁷. For spectroscopic

data reduction, all data were reduced with standard routines in IRAF.

II. Light curve fitting and K-correction

Considering the limited understanding of spectral features during the early optical flash phase of MUSSES1604D, we adopt different methods to derive the rest-frame light curves at flash and post-flash phases respectively. For the post-flash light curves, we firstly fit the observed light curves by applying the SALT2 model of SNe Ia spectrophotometric evolution which is built using a large data set including light curves and spectra of both nearby and distant SNe Ia¹⁶. After light curve fitting, K-correction is performed for the rest-frame B - and V -band light curves according to the best-fitting spectral sequence model of MUSSES1604D with SNCosmo³⁸. For the light curve in the flash phase (within 5 days after the explosion), we applied the color-based K-correction with a pseudo power-law spectral energy distribution (SED) function $f(\nu) = k\nu^\alpha$, where k and α are parameters derived by the early color information of MUSSES1604D. Considering there is no indication of Na I D absorptions in any of our spectra ($S/N \sim 18$ per resolution element near the wavelength of Na I D lines for the around-max spectrum) and the supernova was located far away from the center of an S0 type host, we only take into account the Galactic extinction of $E(B - V)_{MW} = 0.0263$ mag (SFD, 1998³⁹) in this paper. The rest-frame B - and V -band light curves are shown in Extended Data Figure 3.

The K-corrected rest-frame light curve of MUSSES1604D indicates a B -band peak absolute magnitude of -18.8 but with $\Delta m_{15}(B) \approx 1.0$ mag, corresponding to a slow-evolving normal-brightness SN Ia according to the Phillips relation¹⁷. The V -band light curve of MUSSES1604D

is consistent with typical normal-brightness SNe Ia, such as SN 2011fe. All photometric data in observer and rest frames are listed in Extended Data Table 1.

III. Explanations for the peculiarities of MUSSES1604D

The “peculiarities” of MUSSES1604D mainly include: **1)** a prominent optical flash with peculiar color evolution at very early time; **2)** the red $B - V$ color evolution in general; **3)** a normal-brightness SN Ia with prominent Ti II absorptions in the around-max spectrum; **4)** a slow-evolving B -band light curve. In this section, we compare different scenarios which may account for such peculiarities and find the best solution.

The companion-ejecta interaction We performed two-dimensional axisymmetric radiation hydrodynamic simulations of the explosions of a WD with a Chandrasekhar mass in binary systems to obtain light curves and spectra resulting from collisions between the ejecta and the companion star (Kutsuna-Shigeyama CEI models^{19,40}). The ejecta are described by the W7 model²⁰. The best-fitting light curves presented in Figure 3 are the expected outcome of an explosion in a binary system with a separation of 2.5×10^{13} cm when we observe this event from the companion side. The companion star is a red giant with a mass of $1.05 M_{\odot}$ (the core mass is $0.45 M_{\odot}$) and a radius of 8.9×10^{12} cm, filling the Roche lobe. The initial mass of the companion was assumed to be $1.50 M_{\odot}$. Although the CEI-induced early flash could be prominent under this condition, we cannot reproduce the early light curves and $B - V$ color evolution of MUSSES1604D because a strong but long-duration flash will be produced after interacting with a red giant which has a more extended envelope^{8,19}. For the spectral

peculiarity (Figure 4), the prominent Ti II lines also contradict the predictions from typical explosion models through the hydrogen-accreting single degenerate channel^{5,20}.

Further comparisons of early-phase light curves with both Kutsuna-Shigeyama (K-S) and Kasen’s (K10) CEI models^{8,19} are presented in panels (a)–(c) of Extended Data Figure 1. Note that K10 predicts brighter early flash than K-S models because it assumes instantaneous thermalization in the shocked matter while K-S models approximately take into account thermalization processes between shocked matter and radiation (cooling of shocked matter by bremsstrahlung). As K10 noticed, the assumption of instantaneous thermalization tends to underestimate the energies of photons and also results in overestimating the emissivity from shocked matter. Therefore, K10 models produce a prominent flash with a low-mass main-sequence companion while K-S models can only marginally produce a comparable early flash with a red-giant companion. Accordingly, K-S models with a main-sequence companion produce an even fainter early flash. Despite the different assumptions in two CEI models, both of the models with an early flash as bright as that of MUSSES1604D predict blue color of $B - V \lesssim 0.1$ in the first 4 days after the explosion, which is incompatible with the observations of MUSSES1604D.

The CSM-ejecta interaction In the double-degenerate progenitor scenario where a SN Ia is generated from the merger of two WDs, a considerable amount of material from the disrupted secondary WD may get pushed out to a large radius^{41,42} and possibly result in an early ultraviolet/optical flash due to the interaction with the ejecta^{9,10}. The strong early light curve enhancement requires a very extended CSM distribution^{10,43}. Regardless of the physical possi-

bility of reaching the CSM distribution under their assumptions, interacting with more extended CSM not only strengthens the early flash but also increases the diffusion time, and consequently results in a bluer and longer flash phase¹⁰. As can be seen in panels (d)–(f) of Extended Data Figure 1, early light curves and color evolution predicted by the CSM-ejecta interaction are apparently different from those of MUSSES1604D. To produce a flash with the comparable brightness to the observed one, the particular blue and slow color evolution is inevitable for the CSM-ejecta interaction even after fine-tuning the CSM scale and the ⁵⁶Ni distribution of the inner ejecta. Therefore, the CSM-ejecta interaction cannot explain the prominent early flash with a red and rapid $B - V$ color evolution observed for MUSSES1604D.

The He-detonation-triggered scenarios Another scenario is the SN Ia explosion triggered by the detonation of the He layer. The He detonation accommodates the radioactive materials as the nucleosynthesis ash. For example, the He detonation on the surface of the Chandrasekhar-mass WD would leave ⁵⁶Ni as a main energy source in this layer with the mass fraction ($X_{56\text{Ni}}$) reaching to $\sim 20\%$ (see below). The diffusion time scale⁴⁴ of this He layer to optical photons is estimated to be $\sim 2 \text{ days} \times (\kappa/0.2\text{cm}^2\text{g}^{-1})^{0.5} (M_{\text{He}}/0.02M_{\odot})^{0.5} (V_{\text{He}}/20,000\text{kms}^{-1})^{-0.5}$. Here, the subscript “He” is used for the quantities related to the He layer, and the He as a dominant element in the layer is assumed to be fully ionized. The decay power at ~ 2 days from the ⁵⁶Ni in the He layer is estimated to be $\sim 2.5 \times 10^{41} \text{ erg s}^{-1} (X_{56\text{Ni}}/0.2) \times (M_{\text{He}}/0.02M_{\odot})$. Therefore, the radioactivity in the He-detonation ash is predicted to produce a prompt flash lasting for a few days with the peak bolometric magnitude of ~ -16 assuming the He mass $M_{\text{He}} \sim 0.03 M_{\odot}$. This scenario roughly explains the nature of the early flash found for MUSSES1604D. For the sub-Chandrasekhar WD, the abundance in the He ash is dominated by the other radioactive isotopes,

^{52}Fe and ^{48}Cr , and they power the early flash. Still, a similar argument as above applies.

The synthetic light curves and spectra expected for the He-shell detonation models are simulated as follows (Figures 2–4). We constructed a series of toy one-dimensional models which mimic the results of DDet hydrodynamic simulations^{13,23}. The density structure is assumed to be exponential in velocity space, where the kinetic energy is specified by the energy generation for the assumed burned composition structure. A stratified structure in the composition and uniform abundance pattern in each layer are assumed, where the distribution of the burning products is set to represent the DDet models²³.

The model structures are shown in Extended Data Figures 5 and 6. Our sub-Chandrasekhar model and the Chandrasekhar model are similar to a typical DDet model and W7 model, respectively, in the mass coordinate. For the Chandrasekhar WD model, we replace a part of ^{56}Ni -rich region by the Si-rich region, leading to a more centrally confined structure than the W7 model. Note that we assume a stable Fe/Ni region in the core of the Chandrasekhar model, the mass of which is taken to be $\sim 0.2 M_{\odot}$ similar to the W7 model. For each model, we run multi-frequency and time-dependent Monte-Carlo radiation transfer calculations⁴⁵, which were updated to include radioactive energy input from the decay chains of $^{52}\text{Fe}/\text{Mn}/\text{Cr}$ and $^{48}\text{Cr}/\text{V}/\text{Ti}$ together with $^{56}\text{Ni}/\text{Co}/\text{Fe}$. The code assumes LTE for the ionization, which is generally believed to be a good approximation in the early phase. For example, in the W7 model, LTE and NLTE simulations yield indistinguishable light curves (except for the U -band) until ~ 25 days after the explosion, corresponding to ~ 5 days after the B -maximum⁴⁶. In addition, we do not include the non-thermal excitation of He; generally He absorption lines are invisible for the DDet

models even with this effect²⁴.

The peculiar early light curve and color evolution as well as the strong Ti II absorptions for MUSSES1604D can be naturally reproduced by the DDet scenario, as shown by the model for the $1.03 M_{\odot}$ WD with $0.054 M_{\odot}$ He (ash) layer in Figure 2–4. We note that the idea that the DDet model predicts the early flash by the radioactive decays of the He ash has been independently proposed by another groupⁱ. Their model, qualitatively similar to our sub-Chandrasekhar model, leads to the early flash and the color evolution in the first few days powered by the decay of ^{52}Fe and ^{48}Cr , as is similar to our model prediction. Their model lacks around/post-maximum light curve and spectral information, therefore further comparison between the two models is not possible. Although the sub-Chandrasekhar DDet model can explain most of peculiarities of MUSSES1604D, it has prominent defects in the resulting fast evolution of the simulated *B*-band light curve (see also refs^{13,23}). Note that the fast decline of *B*-band light curve predicted by this classical DDet scenario of the sub-Chandrasekhar-mass WD happens from ~ 17 days after the explosion, and the magnitude becomes ~ 1.4 mag fainter than the peak at $t \sim 25$ days. The difference between the LTE and NLTE treatments in the first 25 days after the explosion is too small to account for such abnormal light curve evolution⁴⁶, and thus it is unlikely that the LTE assumption accounts for this discrepancy. Another issue is that the quantity of radioactive isotopes ($0.054 M_{\odot}$ of the He layer as a minimal He shell for the He detonation) produces a stronger flash than that of MUSSES1604D, which indicates the observationally required amount of the He layer is smaller. For further investigation of the classical DDet scenario, we ran a grid of models spanning WD masses between ~ 0.9 and $1.4 M_{\odot}$, but all the models predict very fast

ⁱThe paper by Noebauer et al.²⁵ was posted on arXiv after we had submitted the original manuscript in which we proposed the same idea based on our own simulations.

evolution in the B -band light curve and/or too bright peak luminosity.

Indeed, this fast evolution in the B -band light curve has been recognized as one of the issues in the (sub-Chandrasekhar) DDet model¹³, since the Fe-peak and Ti/Cr in the He ash should start blocking the photons in the bluer bands once the temperature decreases after the maximum light, and this argument is not sensitive to the LTE or NLTE treatment. It has been shown that this problem would be remedied if the mass of the He layer is much smaller than the classical DDet Model so as not to provide a large opacity^{29,30,47}, partly based on an idea that such a small amount of He ($< 0.01 M_{\odot}$) would lead to the detonation when a substantial fraction of carbon is mixed in the He layer⁴⁸. We have also confirmed from our model sequence that the light curves of sub-Chandrasekhar DDet models are indeed roughly consistent with normal (but relatively faint and fast-evolving) SNe Ia, once the He layer would be removed. However, this scenario would not explain MUSSES1604D, as we do see prominent early flash and signatures of the He ash in the maximum spectra.

To remedy the abnormal fast-evolution issue in the classical DDet scenario, we investigated additional models in which we allow that the relation between the WD mass and the final ^{56}Ni production expected in DDet is not necessarily fulfilled. By coordinating combinations of the WD mass, $M(^{56}\text{Ni})$, and the He mass, the most straightforward choice we found is shown in Figures 2–4, where the models with $1.38 M_{\odot}$ WD, $0.01\text{--}0.03 M_{\odot}$ He-ash layer, and $0.43 M_{\odot}$ of ^{56}Ni are presented. Additionally we investigated the model with $1.28 M_{\odot}$ WD, $0.013 M_{\odot}$ He-ash layer, and $0.44 M_{\odot}$ of ^{56}Ni . While such a relatively less massive WD model can also give a slow-evolving light curve, the pre-maximum $B - V$ color turns out to be too red. Therefore, we

constrain the acceptable WD mass range between 1.28 and 1.38 M_{\odot} . In addition, an even better consistency of the light curves and color evolution from ~ 5 days after the B -band maximum could be expected for our preferred model (1.38 M_{\odot} WD + 0.03 M_{\odot} He-shell) once the NLTE effects were taken into account⁴⁶.

From these analyses, we suggest two scenarios that involve He detonation. First is the He-ignited violent merger scenario¹⁴. In this case, the primary WD mass should still be $\sim 1 M_{\odot}$ to produce the peak luminosity. The accretion stream of He during the merging process may trigger a detonation even if the He mass is small^{14,27}. If the secondary is swept up by the ejecta, this would explain the slow-evolving light curve. However, there are two drawbacks to this scenario. (1) Whether the core detonation can be triggered by the thin-He-shell detonation^{26,27}, and (2) it will involve fine-tuning of the merging configuration (e.g., masses of the WDs) to reproduce the observational features of MUSSES1604D.

The other scenario is the He detonation on the surface of a nearly Chandrasekhar-mass WD, as is motivated by our light curve and spectral models which reproduce the observational results quite well by simply assuming the standard Chandrasekhar-mass WD without fine-tuning. The amount of He mass is also consistent in this picture to trigger the detonation there. The evolutionary track of this binary system toward the He detonation on the surface of a WD more massive than 1.3 M_{\odot} has been never discussed in the literature. Further investigations are needed to explore whether this scenario can be realized or not. Another drawback is that in the classical DDet scenario it will produce too much ^{56}Ni by the core detonation, resulting in an over-luminous SN Ia. Still, the fact that this simple model explains all the main features of

MUSSES1604D is striking, indicating that it is unlikely to be a mere coincidence. This would suggest that there could be a mechanism to reduce the mass of ^{56}Ni as compared to the classical DDet picture.

A more realistic light curve and spectra might be different if one takes into account the possible viewing-angle effect related to both the violent merger scenario and the He-ignited near-Chandrasekhar-WD scenario. Our one-dimensional models only address an angle-averaged behavior. The Ti/Fe absorptions will be stronger than our one-dimensional prediction if the line of sight intersects a region of the He ash. The initial light curve enhancement would also be dependent on the viewing angle, but this effect would be much less prominent than in the absorption.

Another issue is that the Si and S features are not very well reproduced. In general, while these features are qualitatively well explained, obtaining quantitatively good fits is an issue even with sophisticated NLTE modeling⁴⁹. We find that these features are also sensitive to detailed composition structure even in one-dimensional simulations. Providing detailed fitting for these features is beyond the scope of this paper, as these are theoretically more uncertain than the features we have analyzed in this paper.

IV. The explosion epoch of MUSSES1604D

Extrapolating the explosion epoch based on the ^{56}Ni -powered light curve is controversial because a considerable “dark phase” between the explosion and the radioactive decay from SN

ejecta may exist for some SNe Ia^{50–53}. For example, the best-observed SN Ia so far, SN 2011fe likely has a one-day “dark phase” though the SN was discovered at the brightness of $\sim 1/1000$ of its peak brightness^{52,54}. More stringent restriction on the explosion epoch not only requires deep-imaging observations but also specific radiation mechanisms at early time to light up the “dark phase”⁵⁵. Thanks to the deep imaging capability of Subaru/HSC and the early flash of MUSSES1604D, the explosion time of MUSSES1604D can be pinpointed.

For the He-detonation-triggered scenario, the early optical flash is produced immediately from the radioactive decay at the surface of the SN ejecta, which is the earliest optical emission except for the almost non-detectable cooling emission from the shock-heated WD soon after the SN shock breakout^{50,56}. Thus, MUSSES1604D was discovered at an earlier phase than any previously discovered SNe Ia. On the basis of an effectively negligible “dark phase” before the early flash and on-surface radioactive isotopes distribution generated from the He detonation, we adopt the classical t^2 fireball model (t is the time since the explosion) for the rising phase of the early flash, assuming that neither the photospheric temperature nor the velocity changes significantly in estimating the explosion epoch of MUSSES1604D. The result indicates that the first observation of MUSSES1604D is at $\sim 0.51_{-0.06}^{+0.08}$ days after the SN explosion. According to the best-fitting light curves derived from the post-flash multi-band photometry (Figure 1), the g -band magnitude reaches the same level of our first observation (25.14 mag) at $t \sim 3$ days, suggesting that a non-negligible “dark phase” may commonly exist for non-flash SNe Ia.

V. The MUSSES1604D-like SNe Ia and their rarity

The rate of He-detonation-triggered SNe Ia can be constrained by estimating the fraction of MUSSES1604D-like SNe Ia. By inspecting over 1,000 SNe Ia from normal to various kinds of subtypes which have at least one good spectrum from about -6 to +12 days after the B -band maximum through published resources and open SN databases^{57,58}, three MUSSES1604D-like SNe Ia (without early-phase observations) have been found. The screening criteria and detailed properties of the MUSSES1604D-like SNe Ia are listed in Extended Data Table 2. In addition to three normal-brightness SNe Ia ($-19.4 \lesssim M_B \lesssim -18.7$) we mentioned here, some subluminous SNe Ia also show good similarities to MUSSES1604D (e.g. 02es-like SNe Ia, PTF10ops and SN 2010lp, which also have slow-evolving light curve and similar spectral features to MUSSES1604D^{59,60}). However, due to insufficient information for conclusive classification, the discussion here focuses on the “top three” MUSSES1604D-like SNe Ia, SN 2006bt, SN 2007cq, and SN 2012df^{61–64}.

Normal-brightness SN Ia, SN 2006bt shows good similarity with MUSSES1604D in both light curve and spectral features except for the Si II $\lambda 5972$ absorption. Because there is no Na I D feature in spectra of SN 2006bt and the SN is far away from the center of an S0/a host galaxy, the absolute magnitude is shown in Extended Data Table 2 without taking into account the host extinction. Well-organized follow-up observations for SN 2006bt indicate early Ti II absorptions, slow-evolving B -band light curve and similar $B - V$ color evolution to MUSSES1604D.

SN 2007cq is classified as another MUSSES1604D-like SN Ia. In particular, the pre-maximum spectroscopy of SN 2007cq shows that prominent Ti II absorptions have been de-

tected from about 6 days before the B -band maximum, which is consistent with the prediction of the He-detonation models^{12,23}. Note that SN 2007cq shows shallower intermediate element absorption features and bluer color than MUSSES1604D, which can be attributed to the larger amount of ^{56}Ni generated from the core explosion for SN 2007cq.

SN 2012df was located at the edge of an S0-like galaxy. The spectrum was taken near the SN brightness peak with an unfiltered absolute magnitude of ~ -18.9 (without extinction correction). Despite the limited observational information for SN 2012df, high spectral similarity between two SNe Ia has been found at a similar epoch (Figure 4). Therefore we classify SN 2012df as a MUSSES1604D-like SN Ia. Comparisons of the spectral evolution and light curves for MUSSES1604D-like SNe Ia are presented in Extended Data Figure 2 and 3 respectively.

For a conservative estimation of the event rate of MUSSES1604D-like SNe Ia, we screen out all subluminal SNe Ia though some of them may have the same origin^{59,60}. Statistically there are 4 MUSSES1604D-like SNe Ia out of ~ 800 SNe Ia with B -band absolute magnitude $\lesssim -18.7$, corresponding to a fraction of MUSSES1604D-like SNe Ia of $\sim 0.5\%$.

The traditional SN Ia classification mainly based on the SN brightness and spectral features will classify MUSSES1604D and iPTF14atg into two peculiar subtypes although both two have strong early light curve enhancements, slow-evolving light curves, prominent Ti II absorptions, similar color evolution and host environments^{7,55}, implying possible intrinsic connection of two SNe⁶⁵. However, whether iPTF14atg is also triggered by the He-shell detonation is still an

open question because the Ti II absorptions and red color of subluminal SNe Ia in post-flash phase can be attributed to the low temperature of ejecta and the lack of early color information prevents us from further comparisons with MUSSES1604D at the flash phase. It is worth noting that the earliest $B - V$ color of iPTF14atg at ~ 5 days after the explosion probably is too red to be explained by both CEI and CSM-ejecta interaction but is in line with the predictions by He-detonation models (Figure 2). As a reference for the future work, in Extended Data Table 2, we list MUSSES1604D-like and iPTF14atg-like candidates selected from different SN Ia branches^{59,60,66–68}. Similarities among these objects may suggest intrinsic connection between a number of SNe Ia in different subtypes.

Data availability. The photometric source data is available in the online version of the paper. Both photometric and spectroscopic data will also be made publicly available on WISeREP3 (<http://wiserep.weizmann.ac.il/>).

Code availability. The post-flash light curve fitting and K-correction are carried out with the SALT2 model and SNCosmo, which are available at <http://supernovae.in2p3.fr/salt/doku.php> & <https://sncosmo.readthedocs.io/en/v1.5.x/> respectively. We have opted not to make the code for the companion-ejecta interaction (CEI) models and the radiation transfer code used to simulate the He-detonation models available because they are not prepared for the open-use. Instead, all the simulated light curves and spectra of the He detonation models shown in this paper are available upon request.

31. Miyazaki, S., *et al.* Wide-field imaging with Hyper Suprime-Cam: Cosmology and Galaxy Evolution, A Strategic Survey Proposal for the Subaru Telescope. 1–30 (2014).

32. Bolton, A. S., *et al.* Spectral Classification and Redshift Measurement for the SDSS-III Baryon Oscillation Spectroscopic Survey. *Astron. J.* **144**, 144 (2012).
33. Shimasaku, K., *et al.* Statistical Properties of Bright Galaxies in the Sloan Digital Sky Survey Photometric System. *Astron. J.* **122**, 1238–1250 (2001).
34. Peng, C. Y., Ho, L. C., Impey, C. D. & Rix, H. -W. Detailed Decomposition of Galaxy Images. II. Beyond Axisymmetric Models. *Astron. J.* **139**, 2097–2129 (2010).
35. The GALFIT software can be downloaded at <https://users.obs.carnegiescience.edu/peng/work/galfit/galfit.html>.
36. Stetson, P. B. DAOPHOT: A Computer Program for Crowded-Field Stellar Photometry. *Publ. Astron. Soc. Pac.* **99**, 191–222 (1987).
37. Doi, M., *et al.* Photometric Response Functions of the Sloan Digital Sky Survey Imager. *Astron. J.* **139**, 1628–1648 (2010).
38. SNCosmo is available at <https://sncosmo.readthedocs.io/en/v1.5.x/>.
39. Schlegel, D. J., Finkbeiner, D. P. & Davis, M. Maps of Dust Infrared Emission for Use in Estimation of Reddening and Cosmic Microwave Background Radiation Foregrounds. *Astrophys. J.* **500**, 525–553 (1998).
40. Maeda, K., Kutsuna, M. & Shigeyama, T. Signatures of a Companion Star in Type Ia Supernovae. *Astrophys. J.* **794**, 37 (2014).
41. Fryer, C. L., *et al.* Spectra of Type Ia Supernovae from Double Degenerate Mergers. *Astrophys. J. Lett.* **725**, 296–308 (2010).
42. Shen, K. J., Bildsten, L., Kasen, D. & Quataert, E. The Long-term Evolution of Double White Dwarf Mergers. *Astrophys. J.* **748**, 35 (2012).
43. Levanon, N. & Soker, N. Early UV emission from disk-originated matter (DOM) in type Ia supernovae in the double degenerate scenario. *Mon. Not. Astron. Roy. Soc.* **470**, 2510–2516 (2017).
44. Arnett, D. Supernovae and Nucleosynthesis: An Investigation of the History of Matter from

the Big Bang to the Present. Princeton University Press (1996).

45. Kasen, D., Thomas, R. C. & Nugent, P. Time-dependent Monte Carlo Radiative Transfer Calculations for Three-dimensional Supernova Spectra, Light Curves, and Polarization. *Astrophys. J.* **651**, 366–380 (2006).

46. Kromer, M. & Sim, S. A. Time-dependent three-dimensional spectrum synthesis for Type Ia supernovae. *Mon. Not. Astron. Roy. Soc.* **398**, 1809–1826 (2009).

47. Sim, S. A., *et al.* Detonations in Sub-Chandrasekhar-mass C+O White Dwarfs. *Astrophys. J.* **714**, L52–L57 (2010).

48. Shen, K. J., & Moore, K. The Initiation and Propagation of Helium Detonations in White Dwarf Envelopes. *Astrophys. J.* **797**, 46 (2014).

49. Nugent, P., Phillips, M., Baron, E., Branch, D. & Hauschildt, P. Evidence for a Spectroscopic Sequence among Type Ia Supernovae. *Astrophys. J. Lett.* **455**, L147–L150 (1995).

50. Piro, A. L., & Nakar, E. What can we Learn from the Rising Light Curves of Radioactively Powered Supernovae? *Astrophys. J.* **769**, 67 (2013).

51. Piro, A. L., & Nakar, E. Constraints on Shallow ^{56}Ni from the Early Light Curves of Type Ia Supernovae. *Astrophys. J.* **784**, 85 (2014).

52. Mazzali, P. A., *et al.* Hubble Space Telescope spectra of the Type Ia supernova SN 2011fe: a tail of low-density, high-velocity material with $Z < Z_{\odot}$. *Mon. Not. Astron. Roy. Soc.* **439**, 1959–1979 (2014).

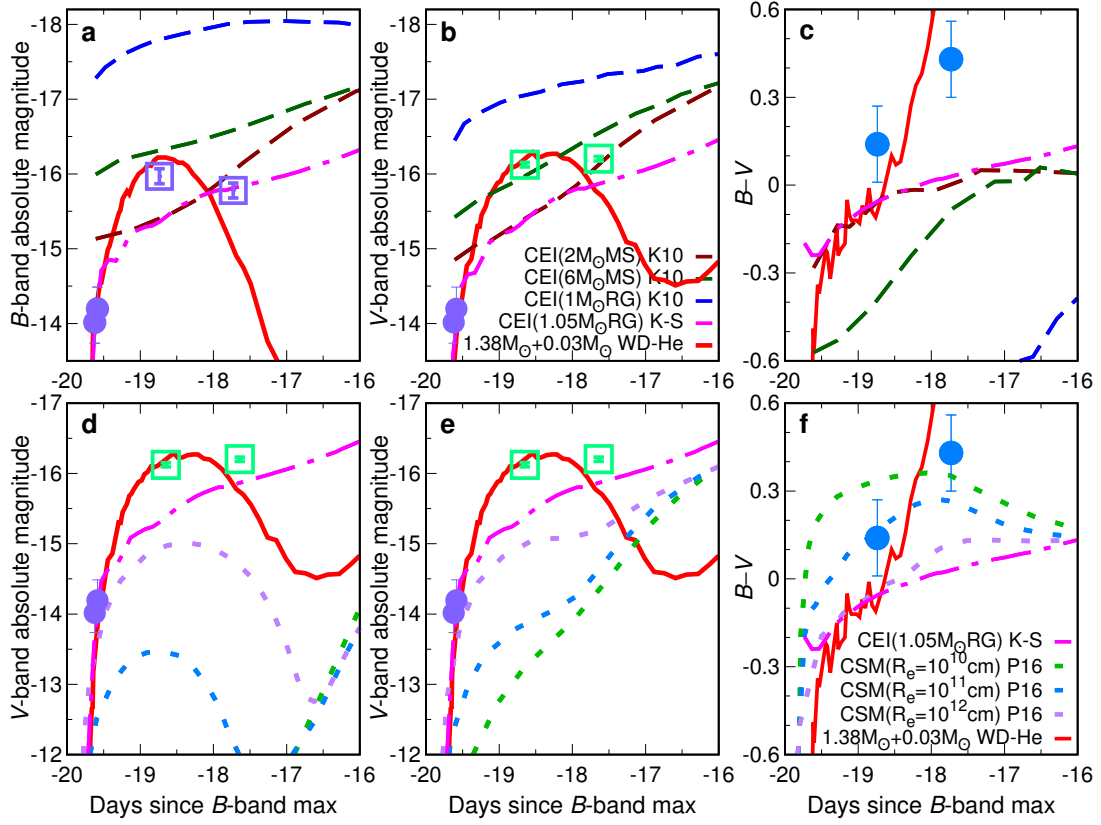
53. Zheng, W., *et al.* Estimating the First-light Time of the Type Ia Supernova 2014J in M82. *Astrophys. J. Lett.* **783**, L24 (2014).

54. Nugent, P. E., *et al.* Supernova SN 2011fe from an exploding carbon-oxygen white dwarf star. *Nature.* **480**, 344–347 (2011).

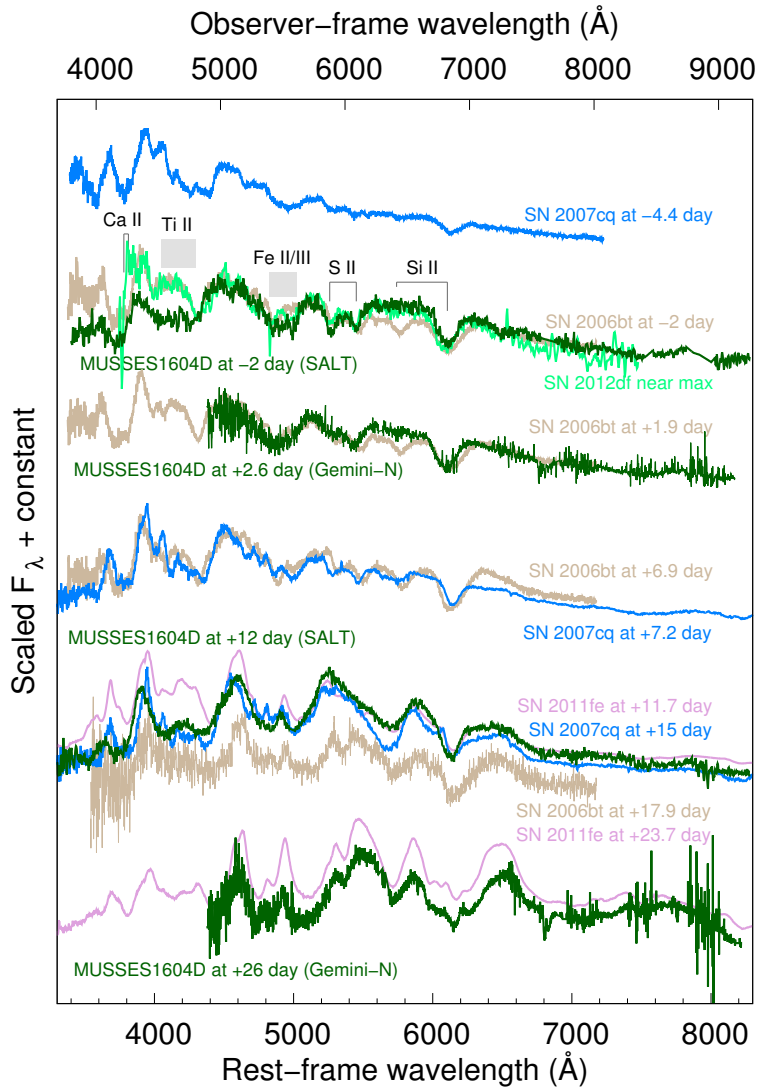
55. Cao, Y., *et al.* SN2002es-like Supernovae from Different Viewing Angles. *Astrophys. J.* **832**, 86 (2016).

56. Piro, A. L., Chang, P. & Weinberg, N. N. Shock Breakout from Type Ia Supernova. *Astrophys. J.* **708**, 598–604 (2010).

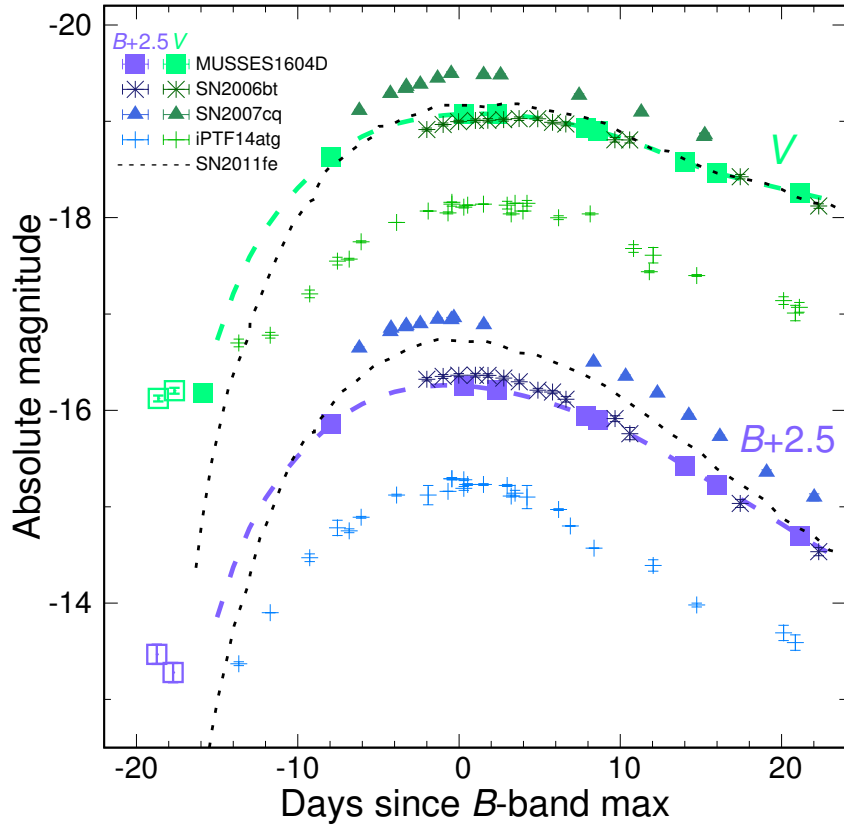
57. Yaron, O. & Gal-Yam, A. WISEREP—An Interactive Supernova Data Repository. *Publ. Astron. Soc. Pac.* **124**, 668–681 (2012).
58. Guillochon, J., Parrent, J., Kelley, L. Z. & Margutti, R. An Open Catalog for Supernova Data. *Astrophys. J.* **835**, 64 (2017).
59. Maguire, K., *et al.* PTF10ops – a subluminous, normal-width light curve Type Ia supernova in the middle of nowhere. *Mon. Not. Astron. Roy. Soc.* **418**, 747–758 (2011).
60. Kromer, M., *et al.* SN 2010lp—a Type Ia Supernova from a Violent Merger of Two Carbon-Oxygen White Dwarfs. *Astrophys. J. Lett.* **778**, L18 (2013).
61. Foley, R. J., *et al.* SN 2006bt: A Perplexing, Troublesome, and Possibly Misleading Type Ia Supernova. *Astrophys. J.* **708**, 1748–1759 (2010).
62. Ganeshalingam, M. *et al.* Results of the Lick Observatory Supernova Search Follow-up Photometry Program: BVRI Light Curves of 165 Type Ia Supernovae. *Astrophys. J. Suppl.* **190**, 418–448 (2010).
63. Scalzo, R., *et al.* Type Ia supernova bolometric light curves and ejected mass estimates from the Nearby Supernova Factory. *Mon. Not. Astron. Roy. Soc.* **440**, 1498–1518 (2014).
64. Ciabattari, F., *et al.* Supernova 2012df = Psn J17481875+5218023. *Central Bureau Electronic Telegrams*. No. 3161 (2012).
65. Kromer, M., *et al.* The peculiar Type Ia supernova iPTF14atg: Chandrasekhar-mass explosion or violent merger? *Mon. Not. Astron. Roy. Soc.* **459**, 4428–4439 (2016).
66. Ganeshalingam, M., *et al.* The Low-velocity, Rapidly Fading Type Ia Supernova 2002es. *Astrophys. J.* **751**, 142 (2012).
67. Li, W., *et al.* SN 2002cx: The Most Peculiar Known Type Ia Supernova. *Publ. Astron. Soc. Pac.* **115**, 453–473 (2003).
68. Foley, R. J., *et al.* Type Iax Supernovae: A New Class of Stellar Explosion. *Astrophys. J.* **767**, 57 (2013).



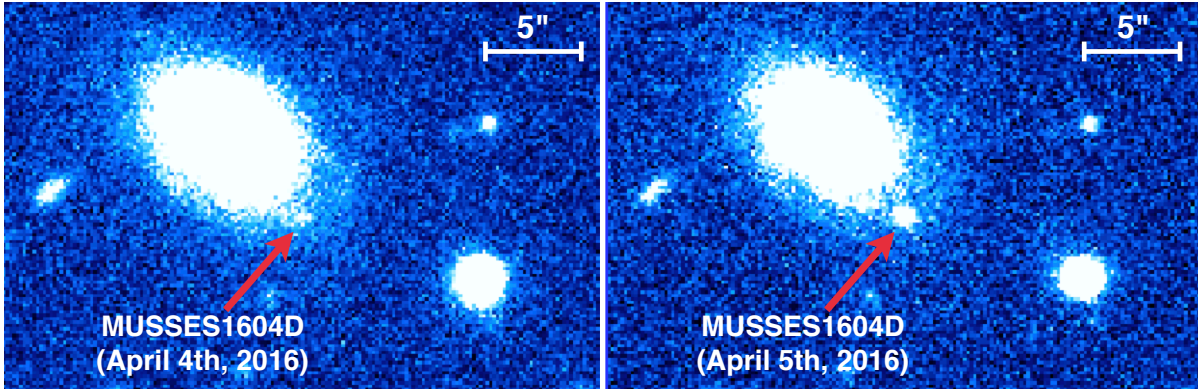
Extended Data Figure 1: Comparison between MUSSES1604D and different models at early phase. Symbols for MUSSES1604D data are the same as those in Figure 1–3 and the results from our best-fitting He-detonation model ($1.38 M_{\odot}$ WD + $0.03 M_{\odot}$ He-shell, red solid lines) are provided in each panel. Panels present the simulated early B -band (a), V -band (b) light curves and $B - V$ color evolution (c) of the companion-ejecta interaction (CEI) observed from the companion side. Dashed lines correspond to the K10 models with different compositions of the binary system⁸. Magenta dash-dot line is our best-fitting K-S CEI model¹⁹. Though an early flash as bright as that of MUSSES1604D could be produced with specific CEI models, the predicted color is very blue at the CEI-flash phase. Panels d and e are V -band light curves simulated by the CSM-ejecta interaction with deep and shallow ^{56}Ni distribution for the inner ejecta respectively (Piro & Morozova, P16¹⁰). Dotted lines correspond to external mass of $M_e = 0.3 M_{\odot}$ with different outer radius R_e . Panel f is the color evolution under the same assumptions as (e). Similar to the CEI models, combinations of early light curves and color evolution predicted by the CSM-ejecta interaction show apparent discrepancies with MUSSES1604D.



Extended Data Figure 2: The spectral evolution of MUSSES1604D and analogs. The spectra of MUSSES1604D (dark green) are compared with analogous SNe Ia, SN 2006bt, SN 2007cq and SN 2012df at similar epochs. Late-phase spectra of SN 2011fe are included for reference. The SALT/RSS follow-up observations were carried out -2 and 12 days after the *B*-band maximum and the other two spectra were taken by Gemini-N/GMOS 3 and 26 days after the *B*-band maximum respectively.



Extended Data Figure 3: The rest-frame B - and V -band light curves of MUSSES1604D and other SNe Ia. K-corrections in flash (open squares) and post-flash phase (solid squares with dashed lines) of MUSSES1604D are carried out with different methods. An excellent light curve match is shown for MUSSES1604D, SN 2006bt and SN 2007cq. Another peculiar early-flash SN Ia iPTF14atg also shows similar light curves though the brightness is ~ 1 magnitude fainter than MUSSES1604D. Light curves of normal SN Ia, SN 2011fe (black dotted lines) are provided for reference. Magnitudes shown here are in the Vega system and the error bars denote $1\text{-}\sigma$ uncertainties.



Extended Data Figure 4: Early Subaru/HSC *g*-band images for MUSSES1604D. Panel **a** shows the earliest Subaru/HSC image of MUSSES1604D ($\alpha(\text{J2000}) = 12\text{h}18\text{m}19\text{s}.85$, $\delta(\text{J2000}) = +00^\circ15'17.38''$) taken on UT 2016 April 4.345, when the *g*-band magnitude of MUSSES1604D was 25.14 ± 0.15 . Then, the SN rapidly brightens to ~ 23.1 mag in one day (panel **b**).

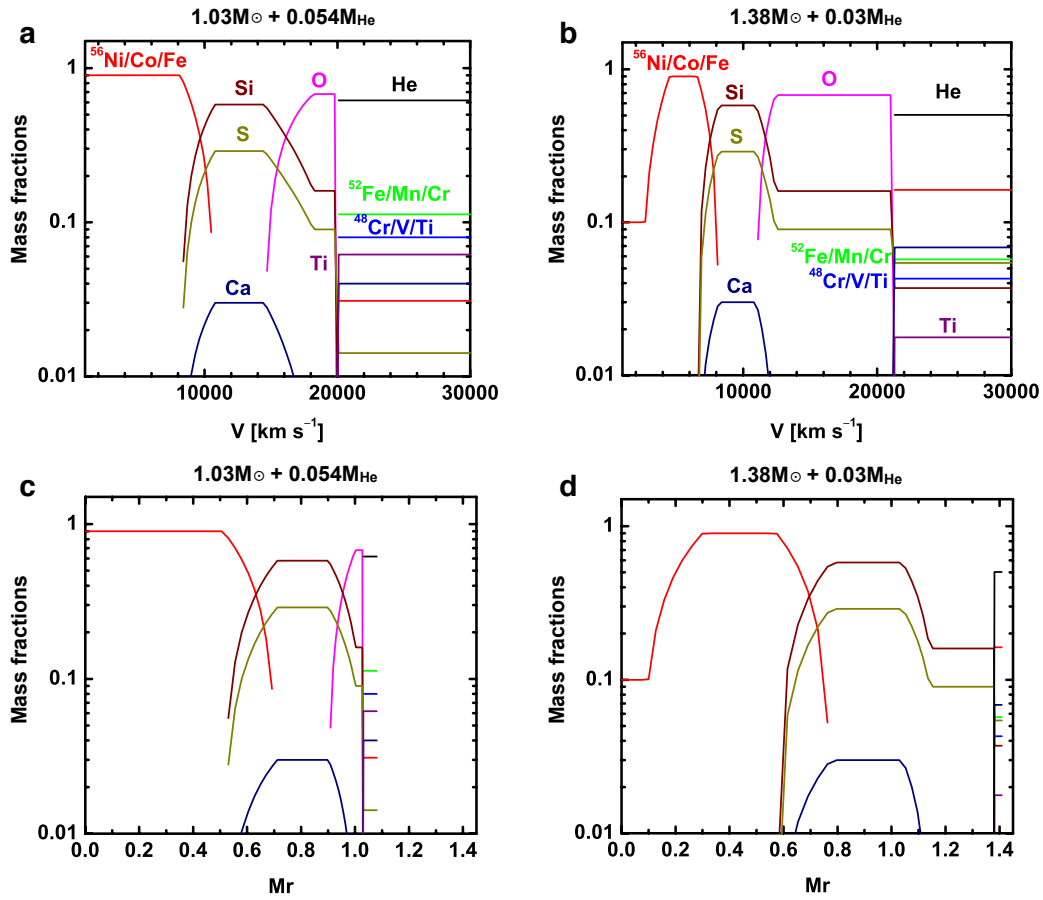
Extended Data Table 1: Imaging observations of MUSSES1604D

UT Date	Phase ^a	Telescope/Instrument	<i>g</i>	<i>r</i>	<i>i</i>	<i>B</i> ^b	<i>V</i> ^b
Apr 04.34	-19.62	Subaru/HSC	25.14 (15)	–	–	–	–
Apr 04.39	-19.58	Subaru/HSC	24.96 (16)	–	–	–	–
Apr 05.25	-18.82	Subaru/HSC	23.09 (07)	–	–	–	–
Apr 05.29	-18.78	Subaru/HSC	23.15 (06)	–	–	–	–
Apr 05.33	-18.74	Subaru/HSC	23.09 (05)	–	–	–	–
Apr 05.34 – 05.43	-18.74 – -18.65	Subaru/HSC	23.08 (05)	22.99 (05)	–	22.71 (10)	22.57 (03)
Apr 05.49	-18.59	Subaru/HSC	–	22.96 (06)	–	–	–
Apr 05.55	-18.54	Subaru/HSC	–	22.91 (05)	–	–	–
Apr 06.46 – 06.56	-17.73 – -17.64	Subaru/HSC	23.05 (05)	22.64 (05)	–	22.91 (10)	22.48 (03)
Apr 08.51	-15.89	Subaru/HSC	–	22.14 (04)	–	–	22.50
Apr 17.41	-7.93	ARC/ARCTIC	20.35 (03)	20.06 (03)	–	20.33	20.06
Apr 26.59	0.29	Kiso/KWFC	–	19.60 (06)	–	19.93	19.61
Apr 28.93	2.38	INT/WFC	19.95 (02)	19.64 (01)	19.84 (01)	19.98	19.61
May 05.07	7.87	NOT/ALFOSC	20.32 (03)	19.81 (02)	20.04 (02)	20.24	19.76
May 05.93	8.64	LT/IO:O	20.39 (02)	19.73 (01)	20.01 (02)	20.29	19.79
May 11.93	14.01	LT/IO:O	20.89 (03)	20.04 (03)	20.30 (04)	20.77	20.11
May 14.14	15.99	ARC/ARCTIC	21.04 (04)	20.15 (02)	20.29 (02)	20.97	20.22
May 19.89 – 19.92	21.14 – 21.16	NOT/ALFOSC	21.63 (06)	20.42 (02)	20.32 (04)	21.49	20.43
May 25.32	26.00	Gemini-N/GMOS	22.01 (02)	20.67 (02)	–	21.93	20.62
May 28.91	29.21	LT/IO:O	22.41 (08)	20.80 (03)	20.55 (03)	22.17	20.78
Jun 06.98	37.33	NOT/ALFOSC	22.69 (04)	21.21 (04)	20.98 (05)	22.68	21.26

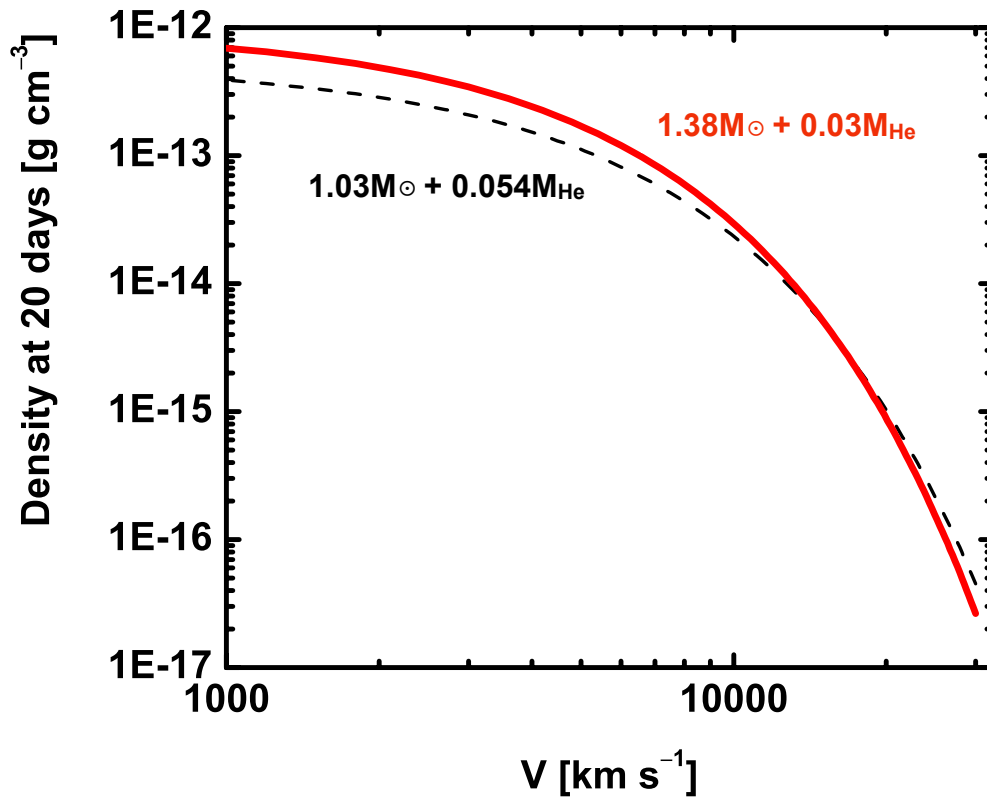
Notes. The magnitudes in *g*, *r* and *i* bands (observer-frame, AB system) have been transferred to the standard SDSS photometric system by adopting the color term correction based on field stars, and rest-frame *B*- and *V*-band magnitudes are in the Vega system. Numbers in parenthesis correspond to 1- σ statistical uncertainties in units of 1/100 mag.

^a Days (rest-frame) relative to the estimated date of the *B*-band maximum, 2016 April 26.27.

^b K-correction for the flash-phase (April 4–8) observations is carried out by using the power-law spectral energy distribution models derived from the color of early flash. For post-flash observations, K-correction is performed according to the best-fitting spectral sequence model of MUSSES1604D. The Galactic extinction ($E(B - V)_{MW} = 0.0263$ mag) has been corrected.



Extended Data Figure 5: The composition structures of the models used for radiation transfer simulations. The composition structures shown here are He-detonation models for the sub-Chandrasekhar-mass WD ($1.03 M_{\odot}$ WD + $0.054 M_{\odot}$ He-shell; panels **a** & **c**) and the Chandrasekhar-mass WD ($1.38 M_{\odot}$ WD + $0.03 M_{\odot}$ He-shell; panels **b** & **d**). The mass fractions of selected elements are shown as a function of the velocity (panels **a** & **b**) and the mass coordinate (panels **c** & **d**). Colors used for selected elements are same for all panels.



Extended Data Figure 6: The density structures of the models used for radiation transfer simulations. The density structures (as a function of the velocity) shown here are He-detonation models for the sub-Chandrasekhar-mass WD ($1.03 M_{\odot}$ WD + $0.054 M_{\odot}$ He-shell; black dashed line) and the Chandrasekhar-mass WD ($1.38 M_{\odot}$ WD + $0.03 M_{\odot}$ He-shell; red solid line).

Extended Data Table 2: Properties of MUSSES1604D- and iPTF14atg-like SNe Ia

SN Name	B_{Max}^a (mag)	$\Delta m_{15}(B)$ (mag)	$B - V$ Level ^b	TiII Absorptions ^{c,d}	SiII $\lambda 5972^{c,e}$	$V_{SiII \lambda 6355}^c$ (km s ⁻¹)	TiII Evolution ^f
MUSSES1604D-Like SN Ia Candidates							
MUSSES1604D	-18.8 ₊	1.0 ₊	Red ₊	Very Deep ₊	Shallow ₊	11,800 ₊	Slow ₊
SN 2012df ₊	-18.9 ^g ₊	—	Marginal-red ₊	Deep ₊	Shallow ₊	12,000 ₊	—
SN 2007cq ₊	-19.4 ₊	1.1 ₊	Normal ₋	Deep ₊	Shallow ₊	11,000 ₊	Slow ₊
SN 2006bt ₊	-18.9 ₊	1.1 ₊	Marginal-red ₊	Deep ₊	Intermediate ₋	11,600 ₊	Slow ₊
SN 2011fe ₋	-19.2 ₊	1.2	Normal ₋	Intermediate ₋	Intermediate ₋	10,300	Normal ₋
iPTF14atg-Like SN Ia Candidates							
iPTF14atg	-17.7 ₊	1.3 ₊	Red ₊	Very Deep ₊	Deep ₊	7,300 ₊	Normal ₊
SN 2002es ₊	-17.9 ₊	1.3 ₊	Red ₊	Very Deep ₊	Deep ₊	6,000 ₊	Normal ₊
SN 2010lp _?	-17.9 ₊	1.4 ₊	Ultra-Red ₊	Very Deep ₊	Deep ₊	10,600 ₋	—
PTF10ops _?	-17.8 ₊	1.1 ₊	Ultra-Red ₊	Deep ₊	Deep ₊	10,000 ₋	Normal ₊
SN 2011ay _?	-18.1 ₊	1.3 ₊	Red ₊	Deep ₊	Intermediate	5,600 ₊	Fast ₋
SN 2008A _?	-17.9 ₊	1.3 ₊	Red ₊	Deep ₊	Intermediate	6,900 ₊	Fast ₋
SN 2005hk _?	-17.7 ₊	1.5	Marginal-red	Deep ₊	Deep ₊	6,100 ₊	Fast ₋
SN 2008ae _?	-17.1	1.4 ₊	Ultra-Red ₊	Deep ₊	Intermediate	7,900 ₊	Fast ₋
SN 2002cx _?	-17.5 ₊	1.2 ₊	Normal ₋	Deep ₊	Intermediate	5,500 ₊	Normal ₊

Notes. For each property, we use “+”, “|” and “-” footnotes as “support”, “neutral” and “opposite” respectively to show the similarity between candidates and MUSSES1604D/iPTF14atg. For all three MUSSES1604D-like SNe Ia, the host extinction are neglected because the relatively far location of SNe to the center of their S0/a host galaxies and the non-detection of Na I D lines in their spectra. Galactic extinction has been applied with $E(B - V)_{MW}$ of 0.1096 and 0.050 mag for SN 2007cq and SN 2006bt respectively.

^a The absolute magnitude for iPTF14atg, 02es-like (SN 2002es, SN 2010lp, PTF10ops) and all normal-brightness SNe Ia are calculated by using cosmological parameters $H_0 = 70.0 \text{ km s}^{-1} \text{ Mpc}^{-1}$, $\Omega_m = 0.30$, $\Omega_\Lambda = 0.70$ and $\Omega_v = 0.00$. In the case of 02cx-like SNe Ia, we adopt the value from the related paper⁶⁸.

^b The $B - V$ color information near the B -band maximum. Here, we define $B - V \geq 0.4 \text{ mag}$, $0.4 \text{ mag} > B - V \geq 0.2 \text{ mag}$, $0.2 \text{ mag} > B - V \geq 0.1 \text{ mag}$, $0.1 \text{ mag} > B - V \geq -0.1 \text{ mag}$ and $-0.1 \text{ mag} > B - V$ as “ultra-red”, “red”, “marginal-red”, “normal” and “blue” respectively.

^c Spectral features at around the B -band maximum. For normal-brightness and subluminal SNe Ia, spectra taken on the closest epoch to $t = -2$ and $t = 0$ (relative to the B -band maximum) are used for the similarity comparisons respectively.

^d The relative strength of Ti II absorptions near the B -band maximum. The strength is relative to normal-type SNe Ia, e.g. SN 2011fe.

^e We define the equivalent width of Si II $\lambda 5972$, $EW(Si_{II \lambda 5972}) < 10 \text{ \AA}$, $10 \text{ \AA} \leq EW(Si_{II \lambda 5972}) < 30 \text{ \AA}$, $30 \text{ \AA} \leq EW(Si_{II \lambda 5972})$ as “Shallow”, “Intermediate” and “Deep” respectively.

^f The relative evolution speed of Ti II absorptions in first 10 ± 2 days after the B -band maximum. The evolution speed is relative to SN 2011fe and iPTF14atg for normal-brightness and subluminal SNe Ia respectively.

^g Unfiltered photometry without considering the Galactic extinction $E(B - V)_{MW} = 0.0393 \text{ mag}$.

Supplementary Information

Acknowledgements The authors thank S. C. Leung and M. Kokubo for helpful discussions. We also thank the staff at the Southern African Large Telescope, the Nordic Optical Telescope, and the Gemini-North telescope for observations and people who carried out follow-up observations which were unfruitful due to weather issue. Simulations for the He detonation models were carried out on a Cray XC30 at the Center for Computational Astrophysics, National Astronomical Observatory of Japan. The work is partly supported by the World Premier International Research Center Initiative (WPI Initiative), MEXT, Japan, Grants-in-Aid for Scientific Research of JSPS (16H01087 and 26287029 for M.D. and J.J.; 26800100 and 17H02864 for K.M.; 6H06341, 16K05287, and 15H02082 for T.S.; 26400222, 16H02168, and 17K05382 for K.N.) and the research grant program of the Toyota foundation (D11-R-0830). S.W.J. acknowledges support from the US National Science Foundation through award AST-1615455. M.D.S acknowledges generous support provided by the Danish Agency for Science and Technology and Innovation realized through a Sapere Aude Level 2 grant, the Instrument-center for Danish Astrophysics (IDA), and by a research grant (13261) from VILLUM FONDEN. The Hyper Suprime-Cam (HSC) collaboration includes the astronomical communities of Japan and Taiwan, and Princeton University. IRAF is distributed by the National Optical Astronomy Observatory, which is operated by the Association of Universities for Research in Astronomy (AURA) under a cooperative agreement with the National Science Foundation. The HSC instrumentation and software were developed by the National Astronomical Observatory of Japan (NAOJ), the Kavli Institute for the Physics and Mathematics of the Universe (Kavli IPMU), the University of Tokyo, the High Energy Accelerator Research Organization (KEK), the Academia

Sinica Institute for Astronomy and Astrophysics in Taiwan (ASIAA), and Princeton University. Funding was contributed by the FIRST program from Japanese Cabinet Office, the Ministry of Education, Culture, Sports, Science and Technology (MEXT), the Japan Society for the Promotion of Science (JSPS), Japan Science and Technology Agency (JST), the Toray Science Foundation, NAOJ, Kavli IPMU, KEK, ASIAA, and Princeton University. The Pan-STARRS1 Surveys (PS1) have been made possible through contributions of the Institute for Astronomy, the University of Hawaii, the Pan-STARRS Project Office, the Max-Planck Society and its participating institutes, the Max Planck Institute for Astronomy, Heidelberg and the Max Planck Institute for Extraterrestrial Physics, Garching, The Johns Hopkins University, Durham University, the University of Edinburgh, Queen's University Belfast, the Harvard-Smithsonian Center for Astrophysics, the Las Cumbres Observatory Global Telescope Network Incorporated, the National Central University of Taiwan, the Space Telescope Science Institute, the National Aeronautics and Space Administration under Grant No. NNX08AR22G issued through the Planetary Science Division of the NASA Science Mission Directorate, the National Science Foundation under Grant No. AST-1238877, the University of Maryland, and Eotvos Lorand University (ELTE). This paper makes use of software developed for the Large Synoptic Survey Telescope. We thank the LSST Project for making their code available as free software at <http://dm.lsst.org>.